Supporting Information

Dual Functions of Lewis Acid-Base Synergy and ZnSe-$CoSe_2$ Heterojunctions toward Stable Solid-State Lithium–Sulfur Batteries

Jiafeng He [1], Shanxing Wang[2*], Leiping Liao [1], and Yuanfu Deng [1, 3*]

[1] The Key Laboratory of Fuel Cell for Guangdong Province, School of Chemistry and Chemical Engineering, South China University of Technology, Guangzhou 510640, China

[2] School of Chemistry and Materials Engineering, Huizhou University, Huizhou 516007, China. E-mail: chsxwang@hzu.edu.cn

[3] Electrochemical Energy Engineering Research Centre of Guangdong Province, South China University of Technology, Guangzhou 510640, China

[*] Corresponding authors: Yuanfu Deng

E-mail addresses: chyfdeng@scut.edu.cn

Supporting Figures and Tables

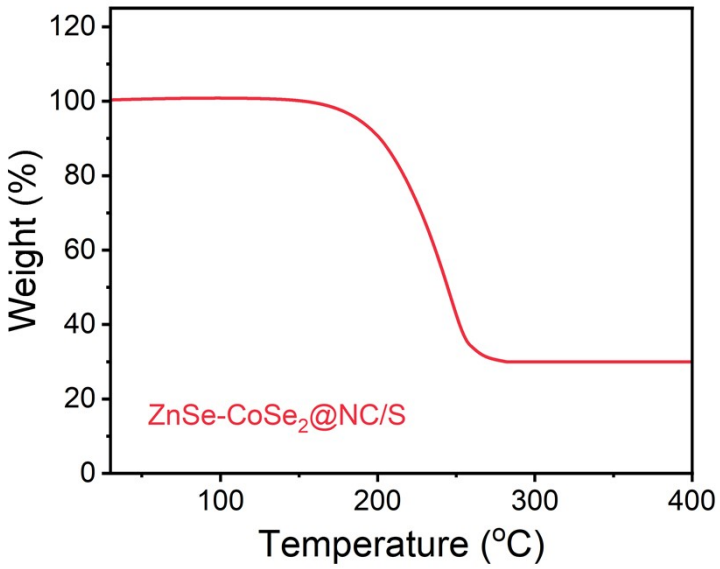

Figure S1. Thermogravimetric analysis curve of the ZnSe-$CoSe_2$@NC/S composite.

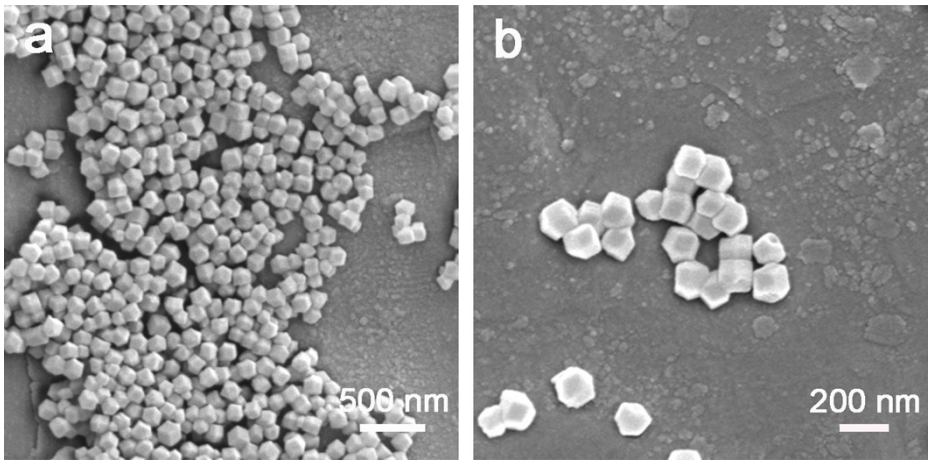

Figure S2. SEM image of ZIF-8 particles.

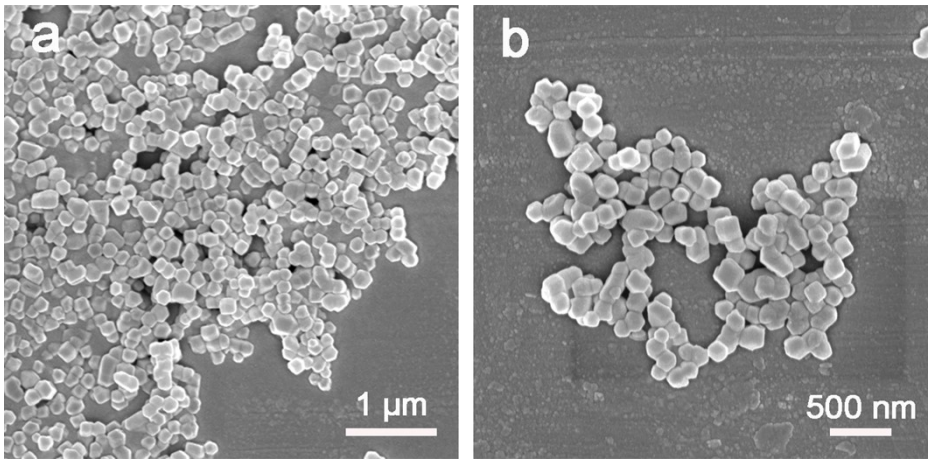

Figure S3. SEM mapping of ZIF-8-ZIF-67.

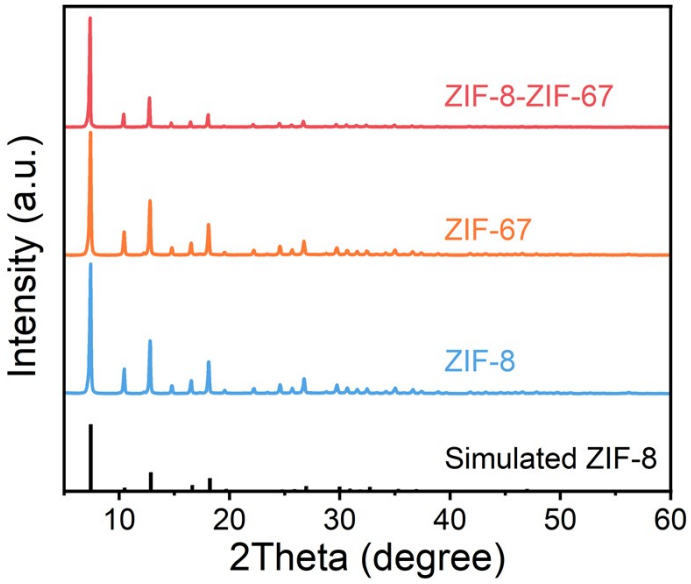

Figure S4. XRD patterns of ZIF-8 and ZIF-8@ZIF-67.

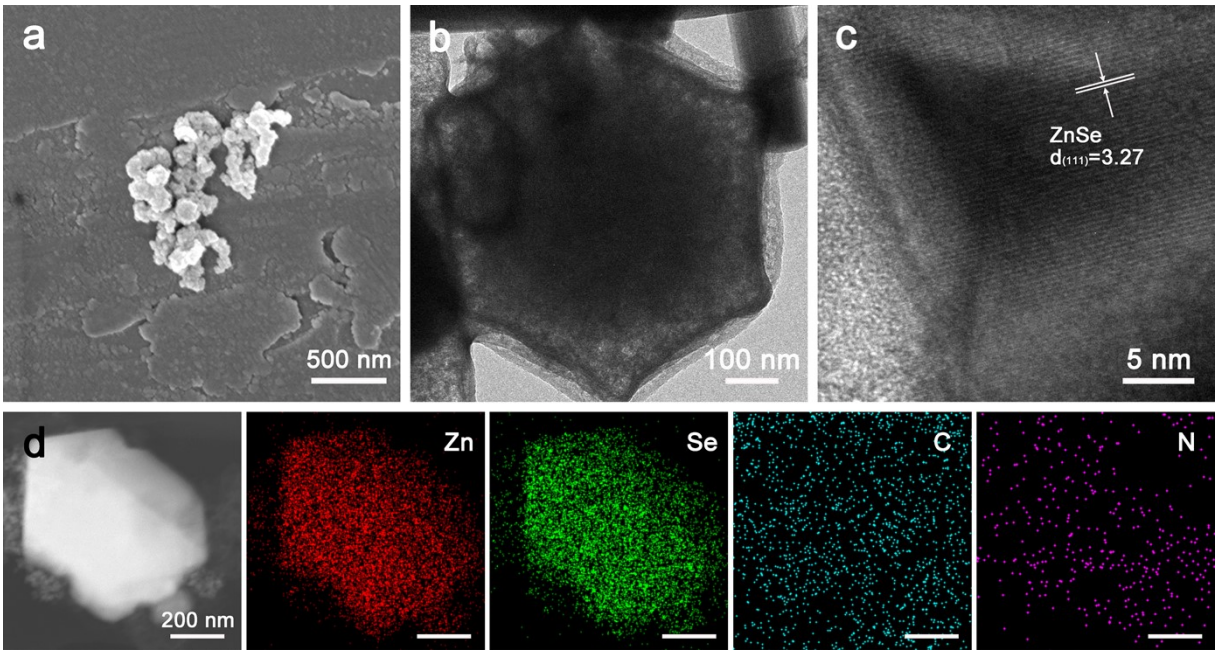

Figure S5. (a) FESEM, (b) TEM, and (c) HRTEM images of ZnSe@NC. (d) HAADF-STEM image and corresponding EDS elemental mapping of Zn, Se, C, and N.

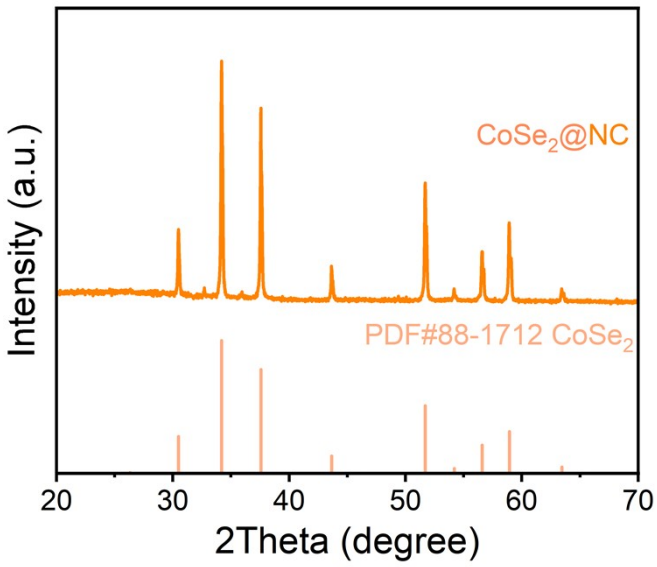

Figure S6. XRD pattern of $CoSe_2$@NC.

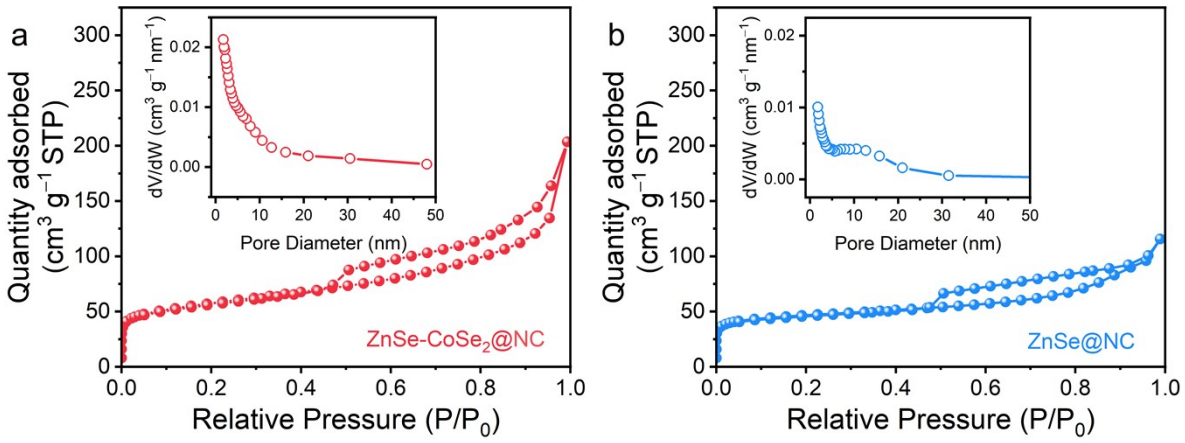

Figure S7. N_2 adsorption-desorption isotherms and pore-size distribution curves (inset) of (a) ZnSe-$CoSe_2$@NC and (b) ZnSe@NC.

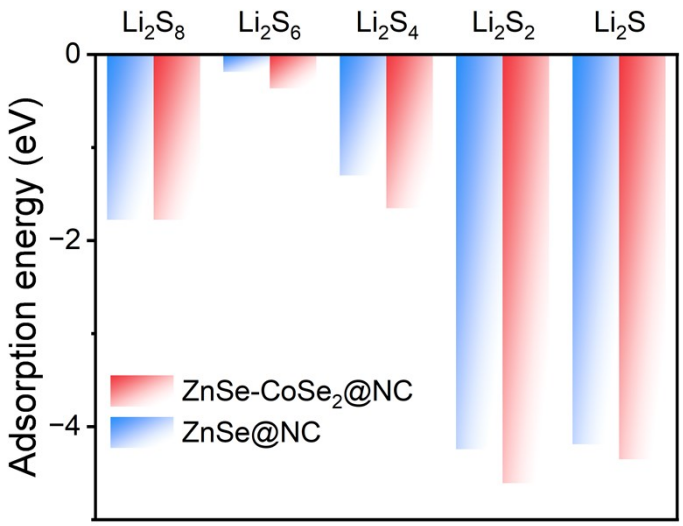

Figure S8. Adsorption energy of ZnSe-$CoSe_2$@NC and ZnSe@NC with LiPSs.

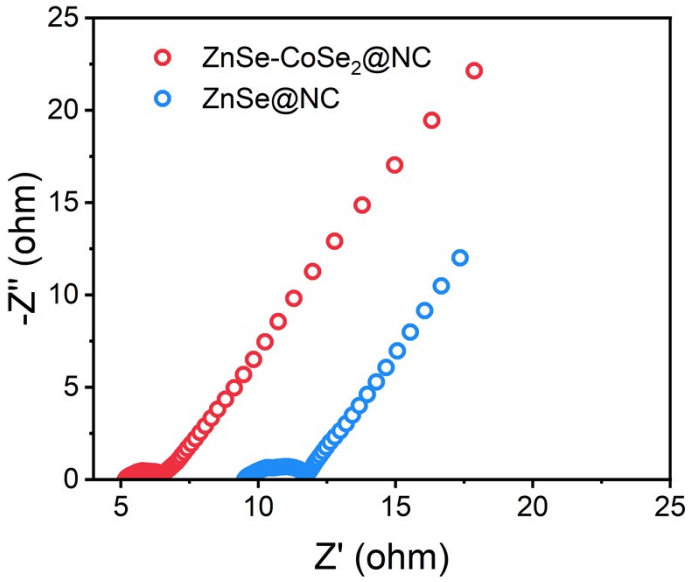

Figure S9. Nyquist plots of symmetric batteries.

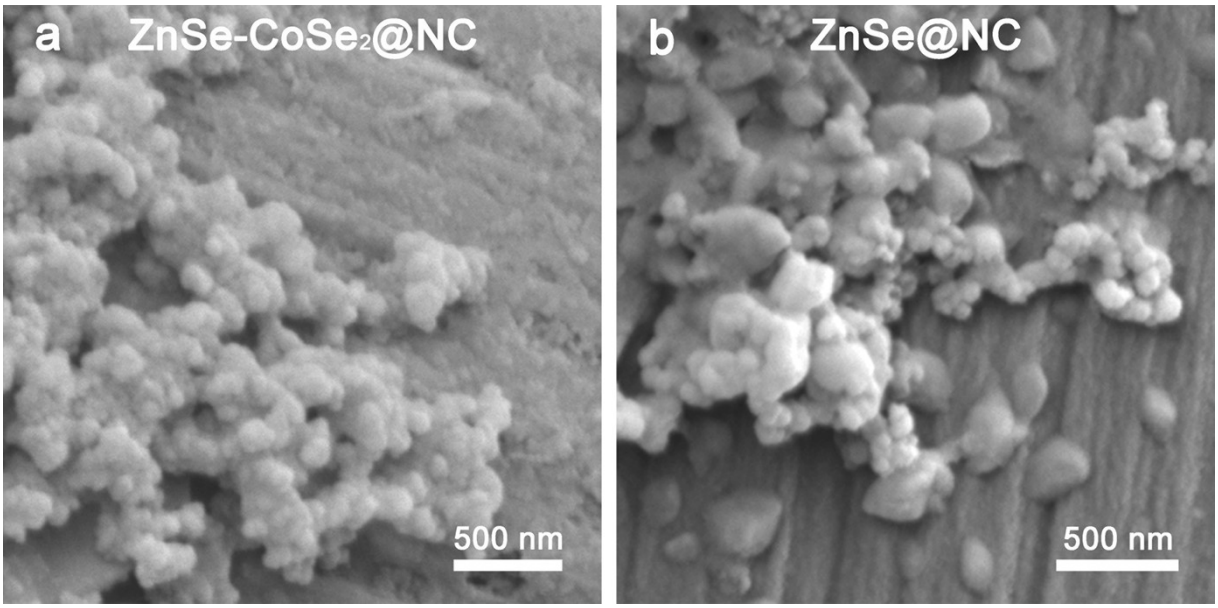

Figure S10. SEM images of (a) ZnSe-$CoSe_2$@NC and (b) ZnSe @NC after Li_2S deposition.

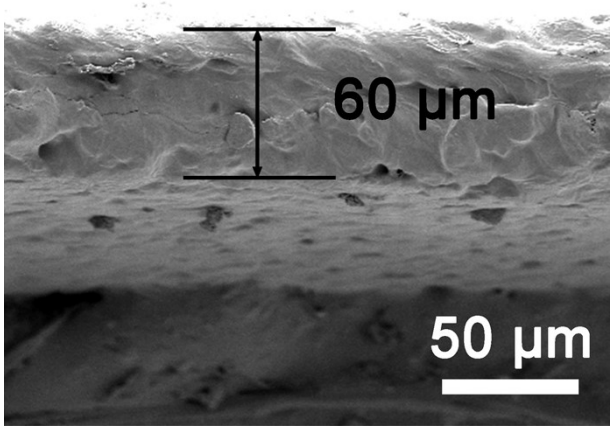

Figure S11. The cross-sectional SEM image of the PVDF-LLZTO film.

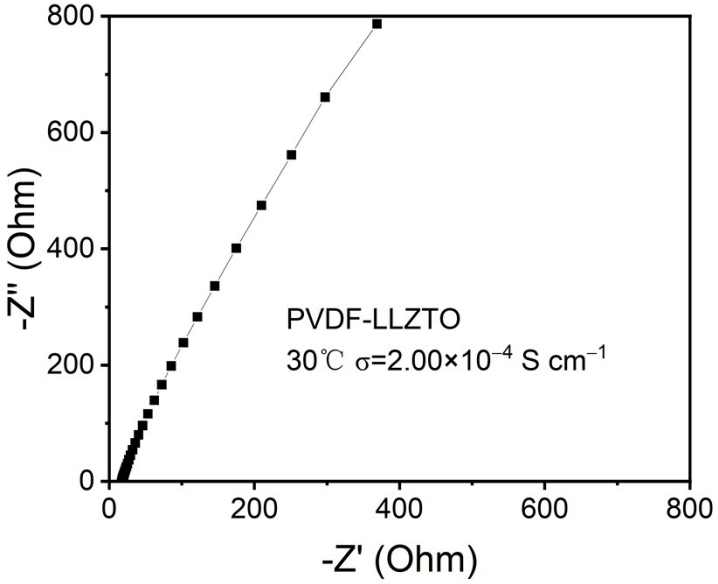

Figure S12. Nyquist plots of PVDF-LLZTO solid-state electrolyte.

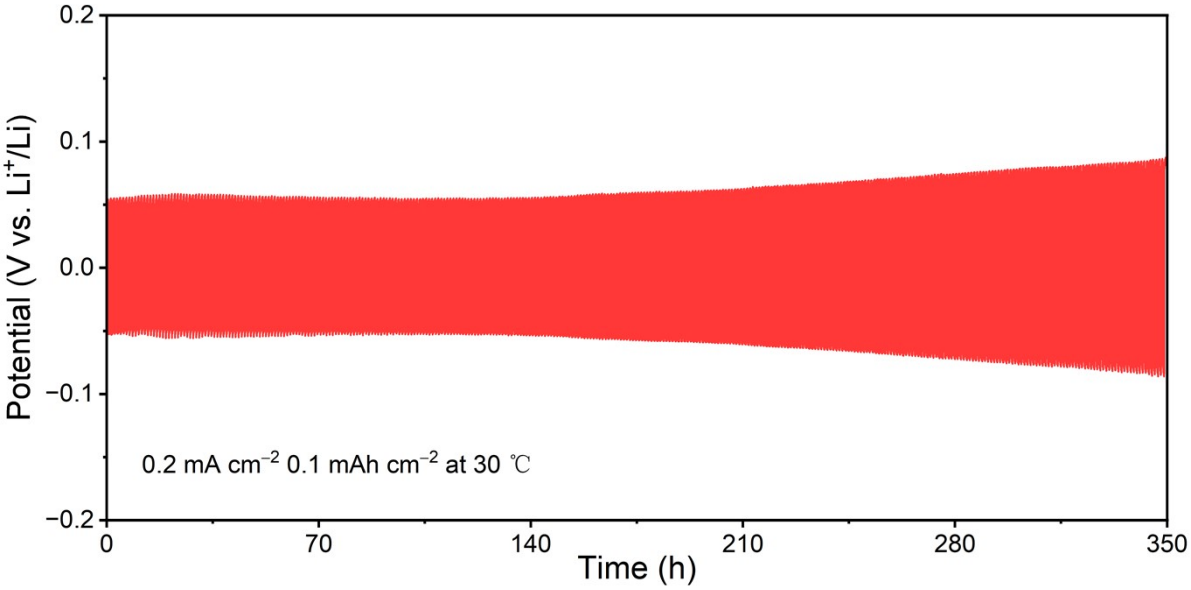

Figure S13. Cycling stability of a Li/ PVDF-LLZTO /Li symmetric cell at 0.1 mA cm^{-2} at 30 °C.

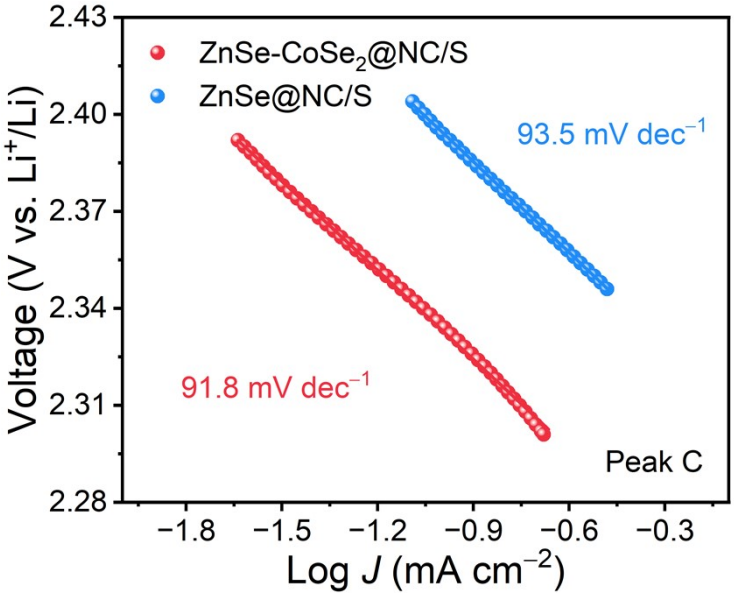

Figure S14. Tafel slopes determined from peak C in Figure 3a.

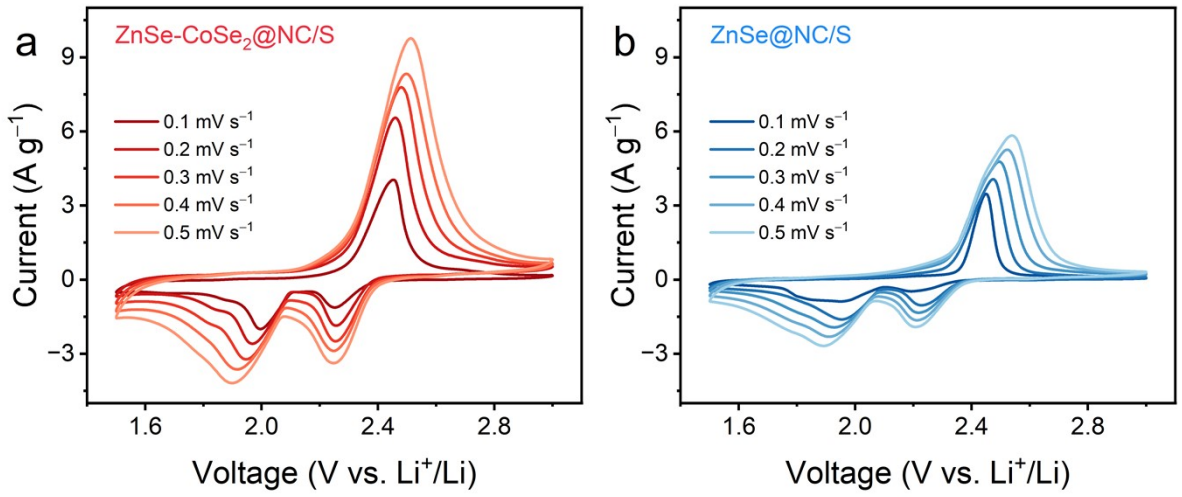

Figure S15. CV curves of (a) ZnSe-$CoSe_2$@NC/S and (b) ZnSe@NC/S electrodes at various scan rates.

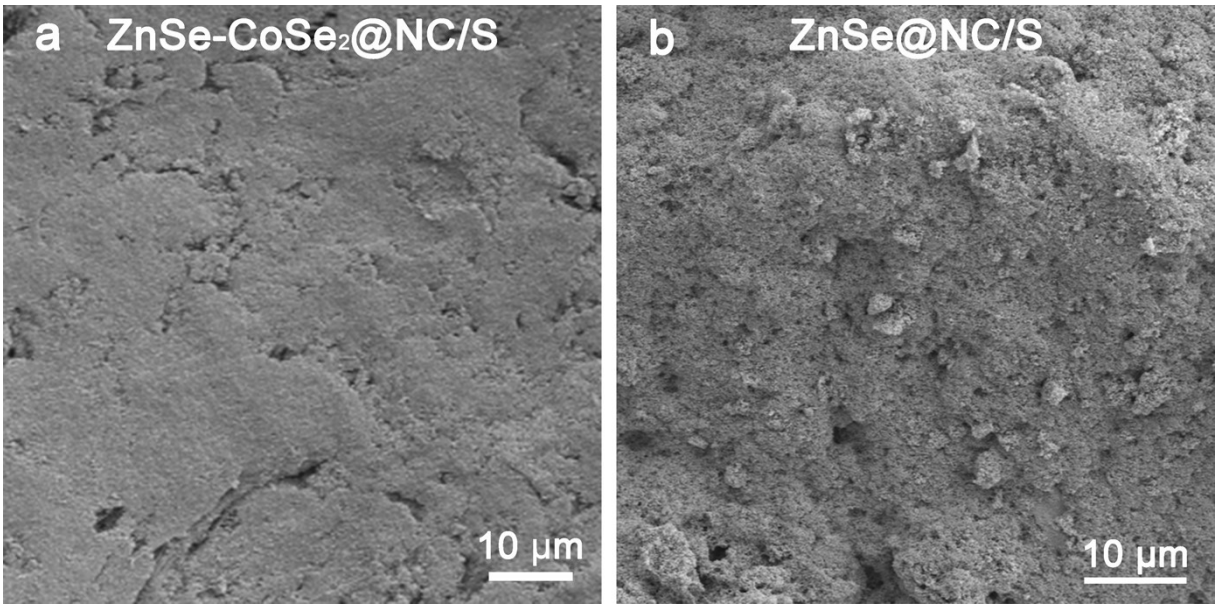

Figure S16. FESEM images of (a) ZnSe-$CoSe_2$@NC/S and (b) ZnSe@NC/S electrodes.

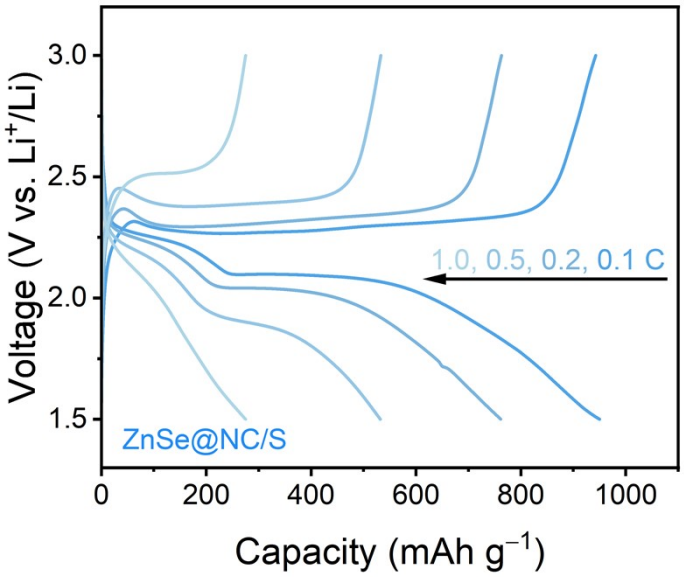

Figure S17. GCD curves of the ZnSe@NC/S electrode at various rates.

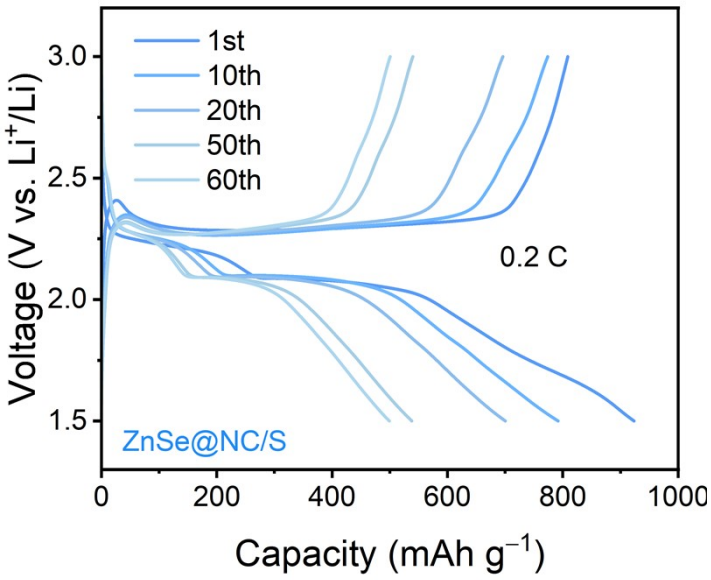

Figure S18. GCD curves of the ZnSe@NC/S electrode at 0.2 C.

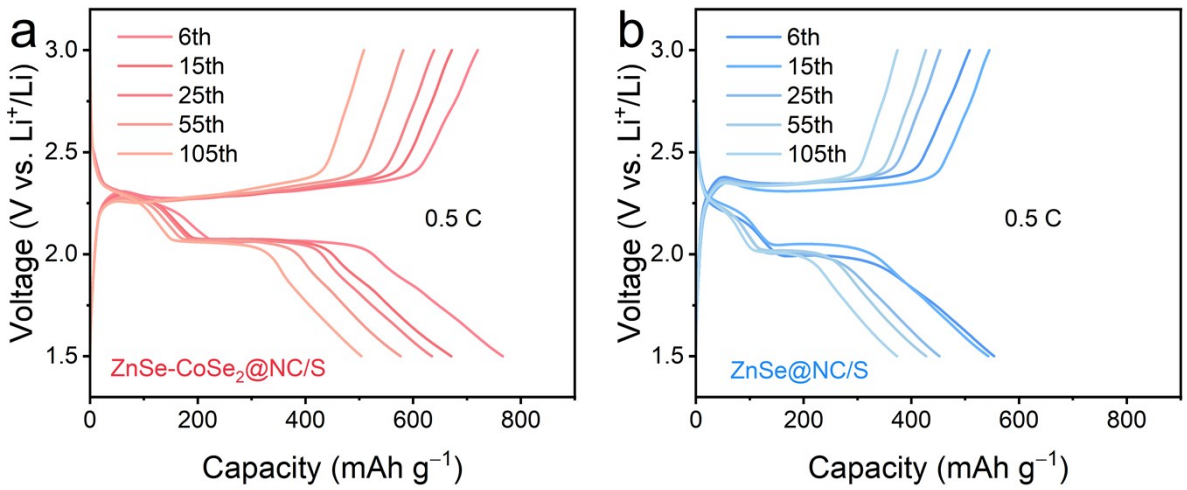

Figure S19. GCD curves of the (a) ZnSe-$CoSe_2$@NC/S and (b) ZnSe@NC/S electrodes at 0.5 C.

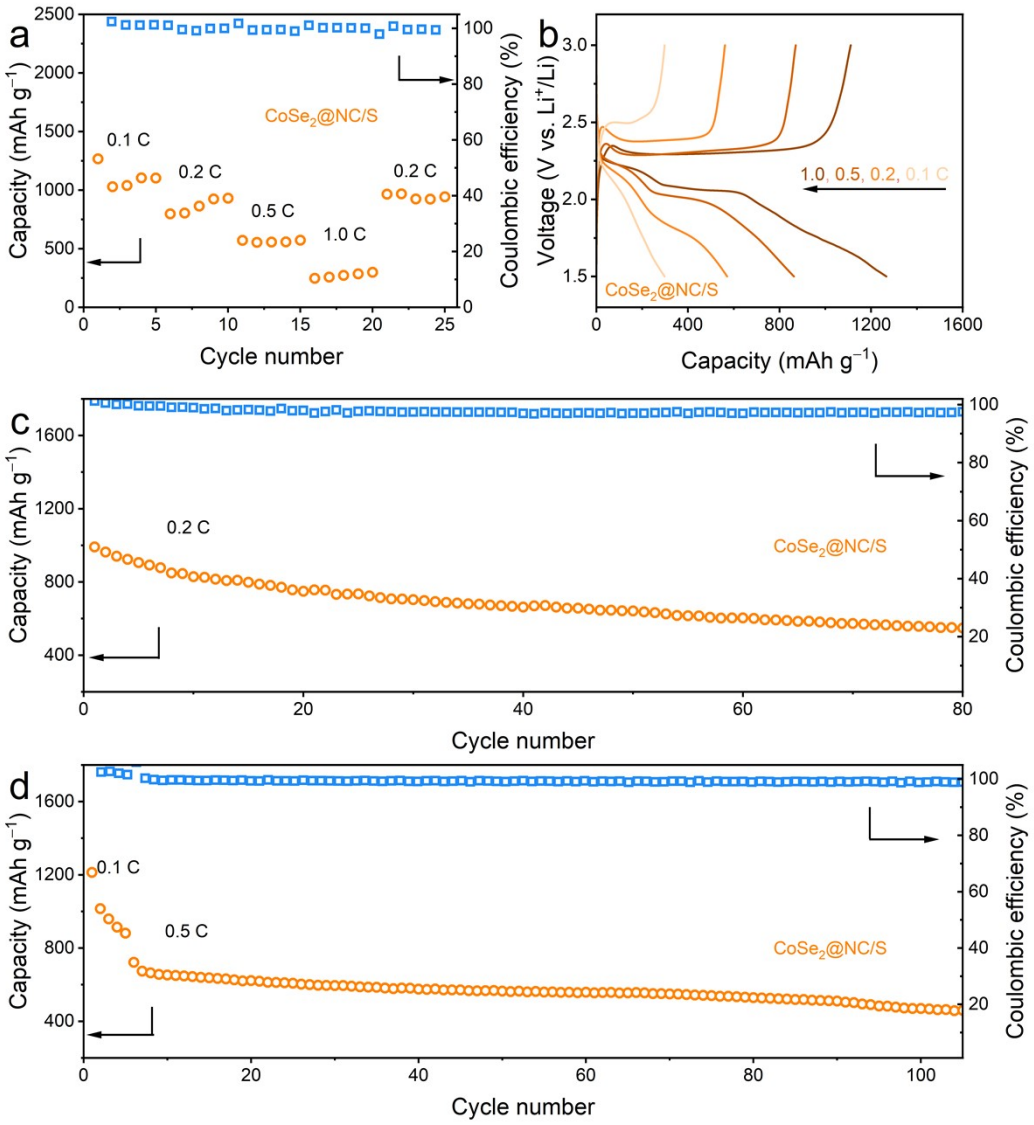

Figure S20. (a) Rate capability, (b) GCD profiles measured at various rates, long-term cycling performance at (c) 0.2 C and (d) 0.5 C of $CoSe_2$@NC/S electrode.

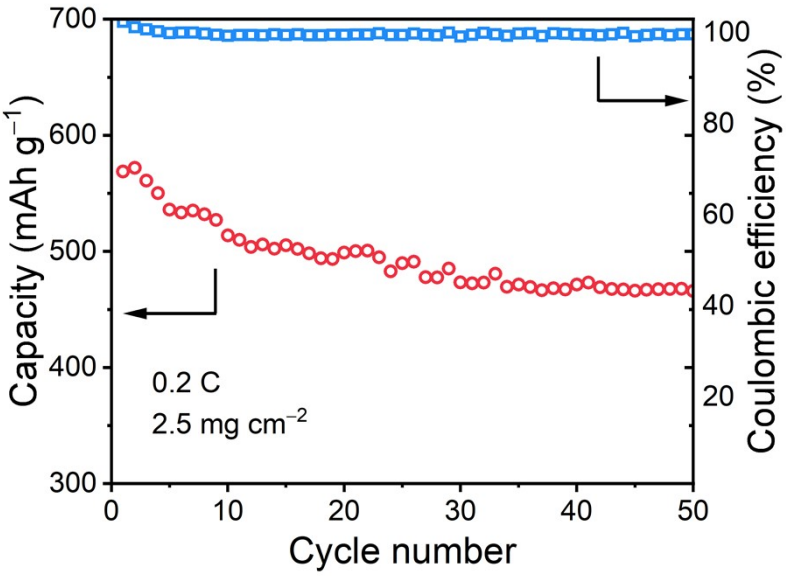

Figure S21. Cycling performance of high-sulfur-loading SSLSB with ZnSe-$CoSe_2$@NC/S electrode at 0.2 C.

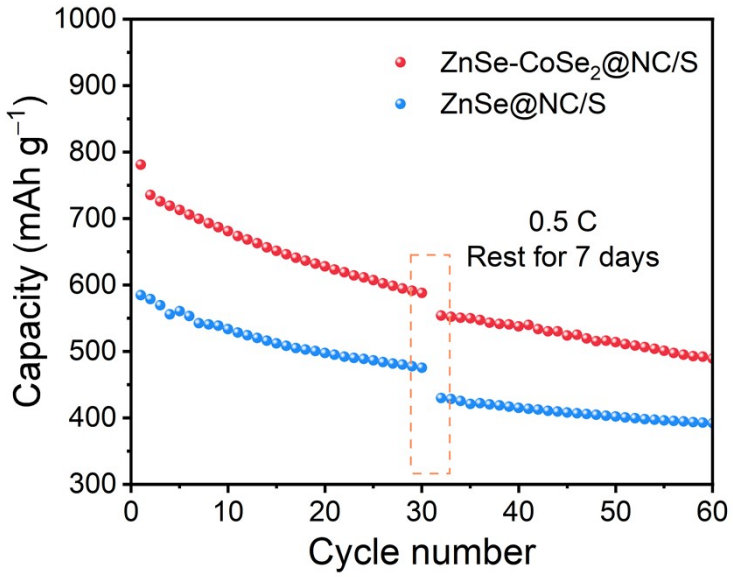

Figure S22. Cycling performance of the SSLSBs at 0.5 C containing an interruption rest for 7 days.

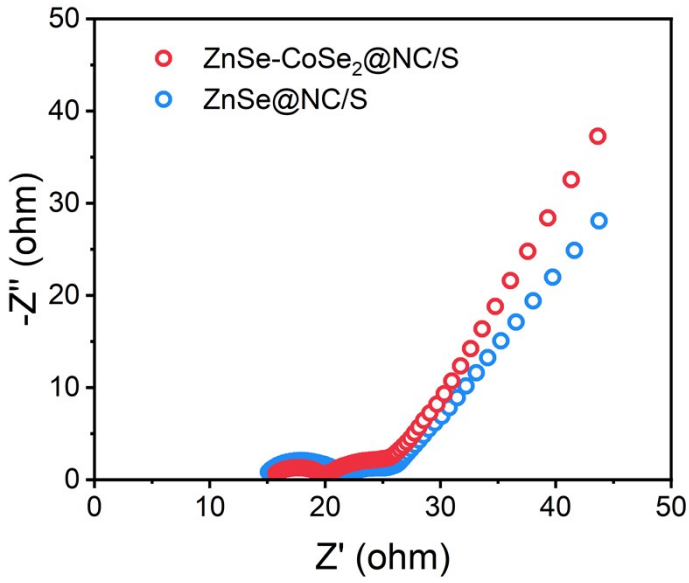

Figure S23. EIS Nyquist plots of SSLSBs assembled with ZnSe-$CoSe_2$@NC/S and ZnSe@NC/S electrodes after cycling.

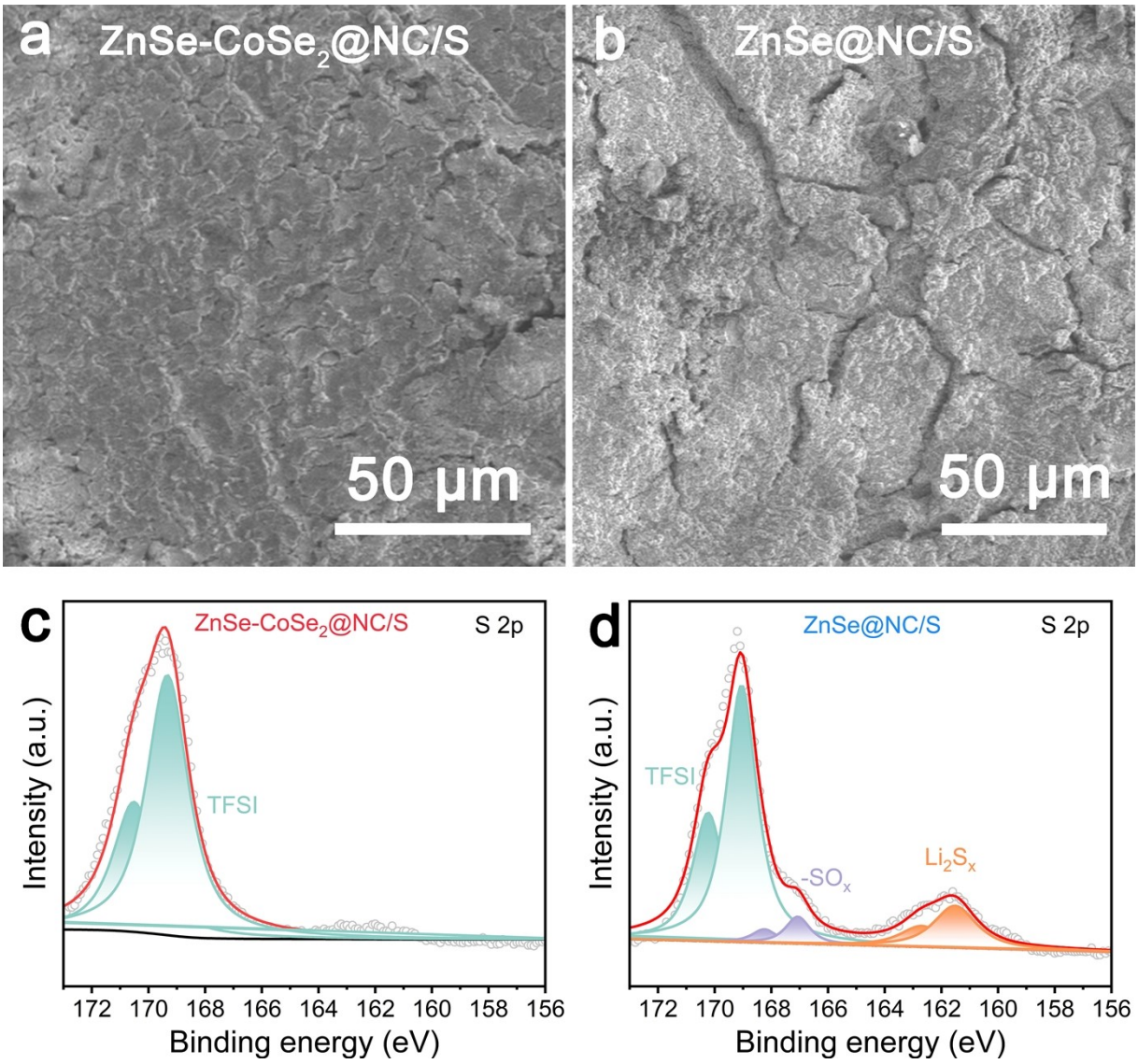

Figure S24. FESEM images of Li anode utilizing (a) ZnSe-$CoSe_2$@NC/S and (b) ZnSe@NC/S electrodes after cycling. High-resolution S 2p XPS spectra of Li anode employing (c) ZnSe-$CoSe_2$@NC/S and (d) ZnSe@NC/S electrodes after cycling.

Table S1. Comparative analysis of the electrochemical properties of recently reported host materials for SSLSBs.

S-cathode components	Composite solid-state electrolytes	*T* / ℃	Current density	Initial capacity (mAh g^{-1})	Cycle number	Retention rate / %	Sulfur loading / mg cm^{-2}	Ref.
KB@S/PEO-LiTFSI	PEO/LiTFSI/MIL-125-NH_2	60	0.1 C	741	50	94.8	0.5-1	[1]
S/KB	PEO-LiTFSI-LLZTO	60	0.2 C	833	50	95.9	0.5	[2]
S@C	PEO-PIM	60	0.2 C	1181	100	61.8	1	[3]
PVDF-Coated Sulfur	PEO/PTFE/LiTFSI	55	0.03 C	818	60	77	1-2	[4]
S/C	PEO-LiTFSI-LLZTO-acetamide	60	0.1 C	980	100	61.2	0.7-0.9	[5]
S/KB	TFSI-QACC/PEO	60	0.1 C	1191.1	100	59	0.5	[6]
S/C	PEO-LiTFSI-Py_{13}TFSI-PGA-Al_2O_3	50	0.2 C	607.9	100	89	1.5	[7]
SPAN	PVDF-HFP-LiFSI	25	0.2 C	1325	100	67.7	0.5-1	[8]
ZnSe-$CoSe_2$@NC/S	**PVDF-LiTFSI-LLZTO**	**30**	**0.2 C** **0.5 C**	**1016** **766**	**80** **100**	**60.6** **65.7**	**0.75-1**	**This work**

Reference

1. J. Li, F. Xie, W. Pang, Q. Liang, X. Yang and L. Zhang, Regulate transportation of ions and polysulfides in all–solid-state Li-S batteries using ordered-MOF composite solid electrolyte, *Sci. Adv.*, 2024, **10**, eadl3925.
2. Y. Liu, H. Liu, Y. Lin, Y. Zhao, H. Yuan, Y. Su, J. Zhang, S. Ren, H. Fan and Y. Zhang, Mechanistic Investigation of Polymer-Based All-Solid-State Lithium/Sulfur Battery, *Adv. Funct. Mater.*, 2021, **31**, 2104863.
3. Y. Ji, K. Yang, M. Liu, S. Chen, X. Liu, B. Yang, Z. Wang, W. Huang, Z. Song, S. Xue, Y. Fu, L. Yang, T. S. Miller and F. Pan, PIM-1 as a Multifunctional Framework to Enable High-Performance Solid-State Lithium–Sulfur Batteries, *Adv. Funct. Mater.*, 2021, **31**, 2104830.
4. R. Fang, H. Xu, B. Xu, X. Li, Y. Li and J. B. Goodenough, Reaction Mechanism Optimization of Solid-State Li–S Batteries with a PEO-Based Electrolyte, *Adv. Funct. Mater.*, 2021, **31**, 2001812.
5. M. Li, Z. Huang, Y. Liang, Z. Wu, H. Zhang, H. Chen and S. Zhang, Accelerating Lithium-Ion Transfer and Sulfur Conversion via Electrolyte Engineering for Ultra-Stable All-Solid-State Lithium–Sulfur Batteries, *Adv. Funct. Mater.*, 2025, **35**, 2413580.
6. C. Ji, S. Wu, F. Tang, Y. Yu, F. Hung and Q. Wei, Cationic cellulose nanofiber solid electrolytes: A pathway to high lithium-ion migration and polysulfide adsorption for lithium-sulfur batteries, *Carbohydr. Polym.*, 2024, **335**, 122075.
7. J. Li, H. Zhang, Y. Cui, H. Da, H. Wu, Y. Cai and S. Zhang, Constructing robust cathode/Li interfaces and intensifying ion transport kinetics for PEO-based solid-state lithium-sulfur batteries, *Chem. Eng. J.*, 2023, **454**, 140385.
8. C. Li, Q. Zhang, J. Sheng, B. Chen, R. Gao, Z. Piao, X. Zhong, Z. Han, Y. Zhu, J. Wang, G. Zhou and H.-M. Cheng, A quasi-intercalation reaction for fast sulfur redox kinetics in solid-state lithium–sulfur batteries, *Energy Environ. Sci.*, 2022, **15**, 4289-4300.